EXPERIMENTAL AND THEORETICAL DEVELOPMENT OF A NEW ISOLATED BOOST DC-DC CONVERTER IN CONTINUOUS CONDUCTION MODE (CCM)

Guillermo Tapia Leiva, Reynaldo Ramos Astudillo and Domingo Ruiz-Caballero

Power Electronic Laboratory - LEP
Electric Engineering School - EIE
PONTIFICIA UNIVERSIDAD CATÓLICA DE VALPARAISO
Av. Brasil 2147, Casilla 4059, Valparaíso, Chile.
domingo.ruiz@ucv.cl

Abstracts – **In this paper the study of a new isolated DC-DC converter in CCM, with two forms to process energy, denominated Flyback-Isolated Boost converter is presented. A qualitative and quantitative analysis in continuous conduction mode is made. Where are obtained the equations that model the behavior of the new converter. The models for their static as well as dynamic behavior are determined; this is made through state-space average method. All the analysis is verified experimentally, through of a design prototype for a power of 200W and working to a frequency of 50 kHz.**

Keywords – **DC-DC converters, Tapped-inductor converters**.

1. INTRODUCTION

It is possible to separate the DC-DC converters between isolated and non-isolated. The main disadvantage of the non-isolated converters, such as: the step-down converter (buck), the step-up (boost), the step-down-up (buck-boost), is the electrical connection between the input and the output. On the other hand, it also is possible to separate them by the way of processing energy; there we have direct and indirect transference. The Buck and Boost converters processes the energy directly, the same happens with all the converters based on these two.

It is different with the Buck-Boost converter and its isolated extension the Flyback converter, both with indirect methods of energy conversion. Nevertheless, the transference in both ways simultaneously was not done by any circuit.

Until Professor A.H. Weinberg developed, a new isolated DC-DC converter, what he called converter with a new principle of energy transference [1] having actually a direct and indirect transference of energy simultaneously.

The objective of Professor Weinberg was to develop an step-up converter that provide with continuous output current, allowing smaller output filters with the resulting weight and size savings. Conventional Weinberg's step-up converter, shown on figure 1(a), is based on this converter.

Other published works show variations to this circuit, such as the new Flyback push-pull converter, shown on [2], and represented by Fig. 1(b). This was an attempt to diminish the number of components and also to be an alternative for conventional Weinberg's converter.

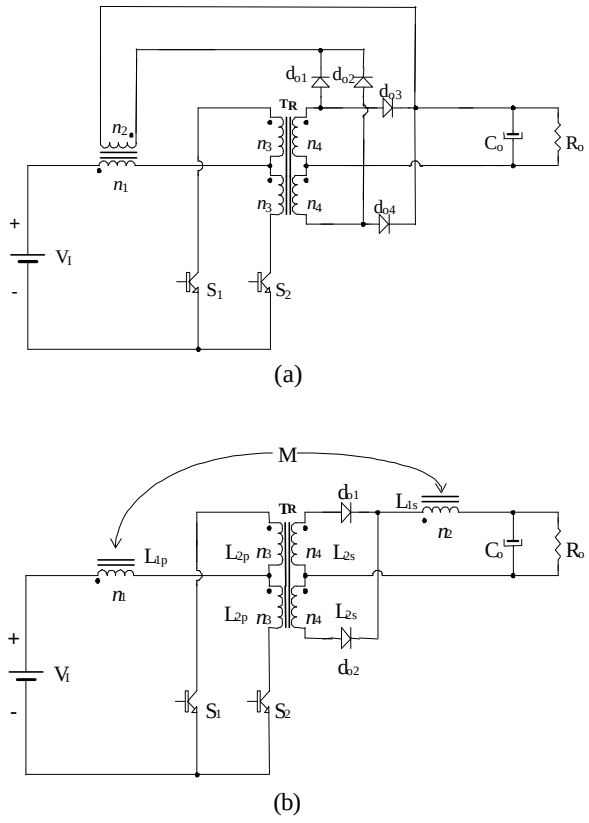

Fig 1 (a) Conventional Weinberg's converter
(b) New Flyback-push-pull converter.

However, this principle of double energy transference, is not exclusive of these converters, also it has been widely used in basic DC-DC converters. This is possible to corroborate with the extensive list of published works [2 – 6].

Figure 2 shows the basic circuits Boost. In this circuit the windings inductor has been replaced by another coupled, being this circuit also known as tapped-inductor Boost converters.

One of the firsts to study this principle applied to the Boost converter was professor Middlebrok [3] during the seventies. Later this was extended to different circuits [5] [6] by others different authors.

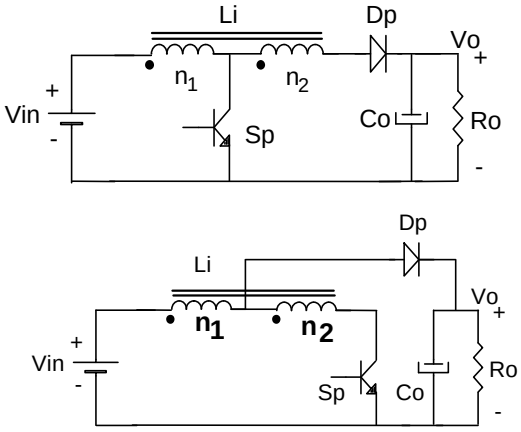

Fig. 2. Tapped-Inductor Boost Converters.

2. PROPOSED CIRCUIT

The proposed circuits are generated applying isolation galvanic to these composed converters with which equivalent isolated circuits are obtained, that will be denominated, from now on, as isolated Flyback-Boost converters, these circuits are shown in figure 3 in their two modalities respectively.

The converter proposed to being studied in this paper, is represented in the figure 3(a). It is constituted by coupled inductors, L_1 and L_2. The disposition of these in the converter, make that when the switch, S_1 is on, this stores energy, and supplying it to the load during the period when S_1 is off. The windings of these coupled inductors are defined the primary as n_1 and the secondary as n_2, hence the ratio of transformation is defined as:

$$N_1 = \frac{n_1}{n_2} \qquad (1)$$

These coupled inductors are separated by a transformer operating in high frequency which provides isolation galvanic between the source and the load, this transformer is known, from now on, as Forward transformer. In addition it provides the direct conversion of energy of the new converter.

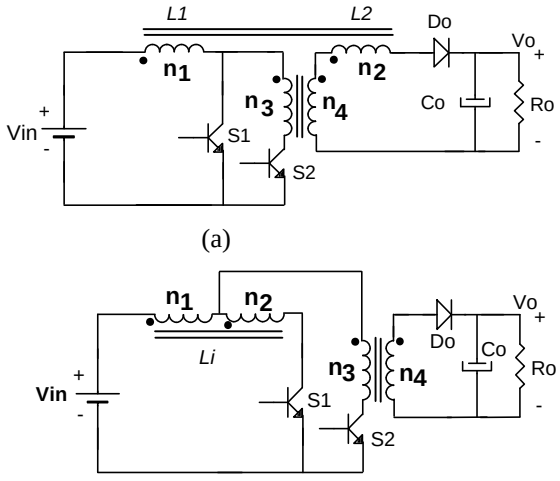

Fig. 3- Circuits generated from the tapped-inductor Boost converter.

The number of turns of the primary of the Forward transformer has been defined as n_3 and the number of turns of the secondary as n_4, hence the ratio of transformation of the Forward transformer is defined by:

$$N_2 = \frac{n_3}{n_4} \qquad (2)$$

Converter also is constituted by an output diode, Do, by two switches of power S_1 and S_2, which provides the characteristic of high frequency to the converter, and finally by an output filters capacitor, Co, which provides voltage constant to the load, filtering the component in high frequency of the output current inductor, generating a current of constant amplitude in the load. The load is represented by an equivalent resistance, Ro.

For the analysis, in continuous conduction mode of the new proposed converter, the following considerations will be had:

- The converter operates in steady state (without any transient).
- All the semiconductors are ideal.
- The Duty cycle, designated as D and defined as D= $\Delta t_1/T$, is greater to 0.5, which generates overlapping pulses of command for the power switches, Figure 5(a) y 5(b).

3. ANALYSIS OF THE NEW CONVERTER.

For the analysis of the new proposed converter it is necessary to take into account the considerations expressed at the final part of second section.

3.1- Flyback-Isolated Boost converter in continuous operation analysis.

There are four operation stages in continuous conduction mode, being these explained in the following paragraphs.

First Stage (Δt_1):

At $t=t_0$, S_2 is commanded to conduct, whereas S_1 is enabled from before stages. In this interval Flyback transformer, through of L1, it continues with the energy storage. Whereas Forward transformer is standing by due to the drive simultaneous of S1 and S2, i.e. the primary voltage V_{L3} is zero in this stage, see figure 4(a). Hence the energy in the load comes from the discharge of capacitor Co.

Second Stage (Δt_2):

At the instant $t=t_1$, the power switch S_1 is turned off, whereas S_2 follows enabled. In this stage the double processing of energy takes place. Direct through Forward transformer and indirect because the Flyback transformer provides the accumulated energy of the previous stages, see figure 4(b). In this stage also the energy stored by primary leakage inductance is sent towards clamping circuit through diode Ds1.

Third Stage (Δt_3):

In this stage S1 is turned on, whereas S2 continues enabled but is not conducting.

This interval is identical to the first. Again, Flyback transformer stored energy and the Forward transformer is standing by due to S1 and S2 are drives simultaneously.

Fourth Stage (Δt_4):

In $t=t_3$ the switch S2 is turned off, whereas S1 continues enabled. In this interval the stored energy in magnetization and leakage inductances of Forward transformer are directed, by diode Ds2, towards the clamping circuit and the primary of Flyback transformer. Therefore, a part of this energy is stored in L1, which increases the total efficiency of the circuit.

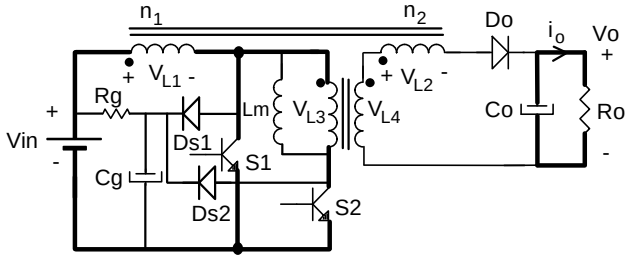

(a) First stage of the converter, Δt_1 interval.

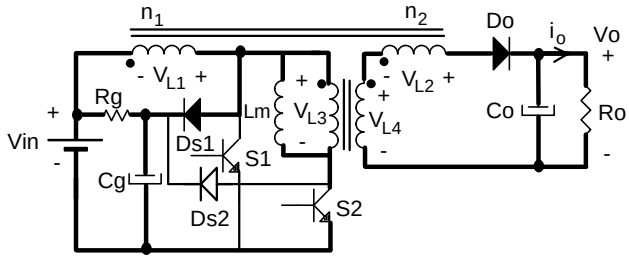

(b) Second stage of the converter, Δt_2 interval.

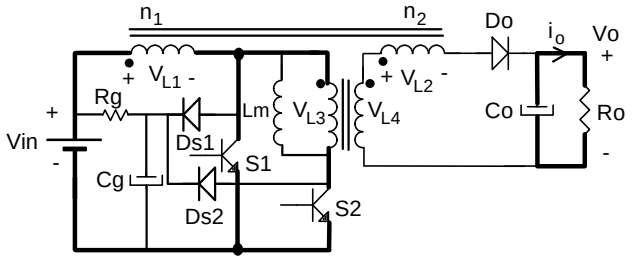

(c) Third stage of the converter,Δt_3 interval.

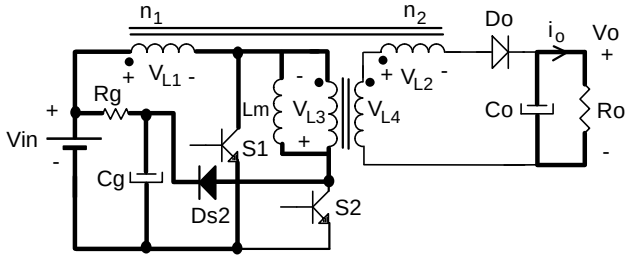

(d) Fourth stage of the converter,Δt_4 interval

Fig. 4- Stages of operation of the Flyback- isolated Boost for half a period of operation.

3.2- Current value in the Δt_1 interval.

In this section it will be possible to obtain the value of the current variation in L_1 respect to the current in the previous interval. See figure 5(c).

It is known that in steady states the inductor flux does not vary in a working period, so the magnetomotriz force contained in the core of the Flyback transformer must be constant. Then it is possible to obtain:

$$f_{mm/\Delta tcond} = f_{mm/\Delta tcond} \tag{3}$$

Equaling this magnetomotriz yields [7]:

$$i_{L1/\Delta tcond} = (1+\frac{N_2}{N_1}) \cdot i_{L1/\Delta tbloq} \tag{4}$$

In equation (5) there is a definition for *K* which is, the times that the current in the interval Δt_2 increases in relation to the current of the previous interval, see figure 5(c).

$$K = 1+\frac{N_2}{N_1} \tag{5}$$

How it can be observed the current-step phenomena appear once again, with the difference in respect with the Flyback-Forward [8], which appears now in the primary circuit current.

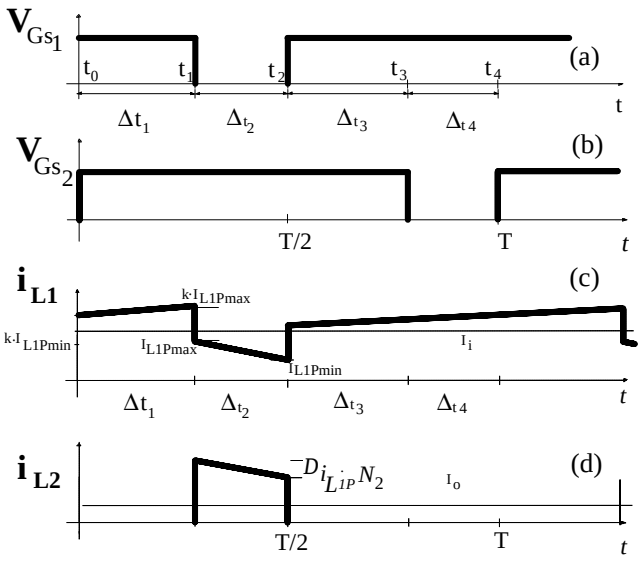

Fig. 5- (a) and (b), command voltages of the switches, (c) Current in the primary, and (d) Current in the secondary of the Flyback transformer.

3.3- Static gain in the continuous conduction mode [7].

In steady state, there is no variation of the flux net in the inductor into a commutation period. Hence the static gain is obtained as:

$$G = \frac{V_s}{V_e} = \frac{(1+D(K-1))}{(N_2 \cdot (1-D))} \tag{6}$$

3.4- Dynamic gain in the continuous conduction mode [7].

In the section further are shows the dynamics gain of the circuit, these are obtained by using the state space average method:

a. -Input-Output Transfer Function (IOTF)

The IOTF is given as:

$$\frac{\hat{v}_s}{\hat{v}_e} = \frac{\dfrac{a \cdot \left(D \cdot (K\text{-}1) + 1\right)}{L_e \cdot C_S}}{s^2 + \dfrac{1}{R_S \cdot C_S} \cdot s + \dfrac{a^2}{C_S \cdot L_e}} \qquad (7)$$

b. -Control-Output Transfer Function (COTF)

The COTF will give us the dynamic system in view of small variations in the duty cycle. This can be seen in the next expression:

$$\frac{\hat{V}_s}{\hat{d}} = \frac{\dfrac{V_e}{Le} \cdot \left[\dfrac{\left[\left(1 + D \cdot (K-1)\right) \cdot N_2 + a \cdot (K-1)\right]}{C_S} - s \cdot \dfrac{\left(1 + D \cdot (K-1)\right) \cdot N_2}{a^2 \cdot R_S \cdot} \right]}{s^2 + \dfrac{1}{R_S \cdot C_S} \cdot s + \dfrac{a^2}{C_S \cdot Le}} \qquad (8)$$

In order to verify the transfer functions found, a number of digital simulations were performed, which are shown on figures 6 and 7. Where is observed the good performances of the models when compared with real circuit, for variations on the input voltage (Fig. 6) or for variations on the duty cycle (Fig. 7).

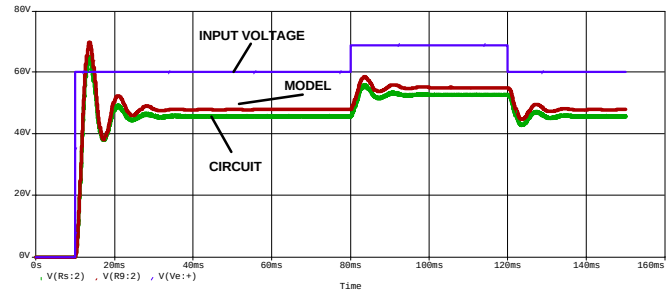

Fig. 6- Disturbances Response in the input voltage.

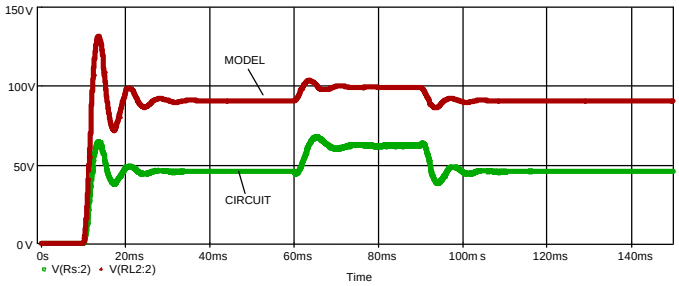

Fig. 7- Disturbances Response in the Duty cycle.

3.5- Ripple in the coupled inductor for the isolated Flyback-Boost converter.

The normalized ripple current in the primary of Flyback transformer, *L1*, is shown in the next expression:

$$\overline{\Delta i_{L1}} = \frac{D \cdot (1 - D)}{K \cdot \left(1 + D \cdot (K-1)\right)} \qquad (9)$$

The ripple of the output current in amperes may be established with the expression shown by equation (10).

$$\Delta i_s = \frac{\overline{\Delta i_{L1}} \cdot N_2^{\,2} \cdot V_s}{F_c \cdot L_1} \qquad (10)$$

4. EXPERIMENTAL VERIFICATION

The parameters to be used in the design of the new isolated Flyback-Boost converter are shown in table 1. The power circuit built is shown in figure 14(a) and its components are shown in table 2. Protection circuits were used for the power switches, which correspond to dissipative snubbers.

The coupling factor of the Flyback transformer and the forward transformer, obtained from the tests, where: 0.998 and 0.9995 respectively.

Next, there are some waveforms experimentally obtained from the built prototype. The figures show different waveforms of the Isolated Flyback-Boost converter, contrasting them with the digital simulations.

In fig. 8 it is possible to observe the current through Flyback transformer primary, showing the current step produced by the transformer ampere-turns.

Fig. 9 shows the voltages across the windings of the Flyback transformer, and in Fig.10 the voltages across the windings of the Forward Transformer, in both cases can be observed that exist a total demagnetization of the cores.

Table 1. Design Parameters.

PARAMETER	DESCRIPTION
Ve = 60 (V)	Input Voltage
Vs = 48 (V)	Output average voltage
Ps = 200 (W)	Output power
D = 0.7	Duty cycle
Fc = 50 (KHz)	Switching frequency
? is = 10% Is	Output current Ripple
$\Delta V_S = 1\% \cdot V_S$	Output voltage Ripple
$h = 0.8$	Converter efficiency
$N_2 = N_1$	Equal ratio transformer

The maximum reverse voltages of the switches are shown by figure 11 and 12. Figure 11 shows for S1, and figure 12 for the switch S2. In both figures are shows the simulation and experimentation waveforms as a way to compare. The voltage in the simulation in S1 and S2 is 330V.

For the experimentation voltages waveforms are obtained 340V for S1 and 280V for S2.

The good performance of the semi-dissipative clamping circuit may be verified on the figure 11. Where could be observed that the clamping voltage was approximately of 340V, giving protection to the switches.

Table 2 - Power circuit components

S_1	IRFP244
S_2	IRFP244
D_1	MUR1510
Dg_1	MUR420
Ds_1	MUR140
Ds_2	MUR140
Cs_1	470[µF] , 100[V]
Cs_2	470[µF] , 100[V]
Cg_S	470[µF], 100[V]
Cg_1	220[nF]
Rg_S	250[O], 5[W]
Rg_1	1[KO],10[W]
Forward Transformer EE-55	Ferrite Core n1=102 turns, 7 wire AWG28 n2=15 turns, 43 wireAWG28
Flyback Transformer EE-55	Ferrite Core n1=39 turns, 13 wire AWG28 n2=6 turns, 27 wire AWG28 lg = 0.068[cm]

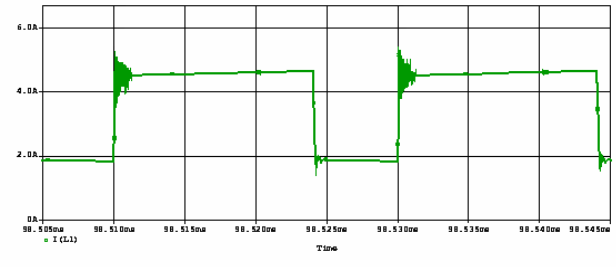

(a)

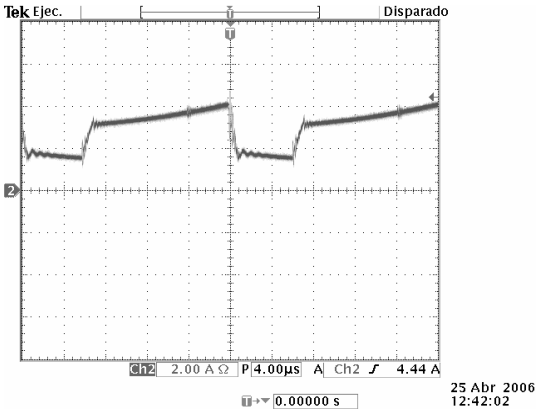

(b)

Fig. 8 (a) Current through of the primary Flyback transformer. Digital simulation.
(b) Primary current of the Flyback transformer. in experimental mode. 2A/div.

Figure 13 shows the output characteristic and the efficiency curve respectively. From the output characteristic, figure 13(a), it is possible to observe the source-voltage behave of the circuit for a given duty cycle.

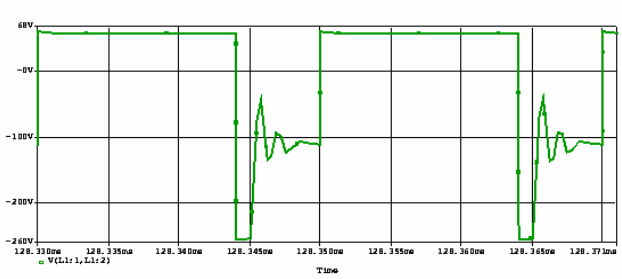

(a)

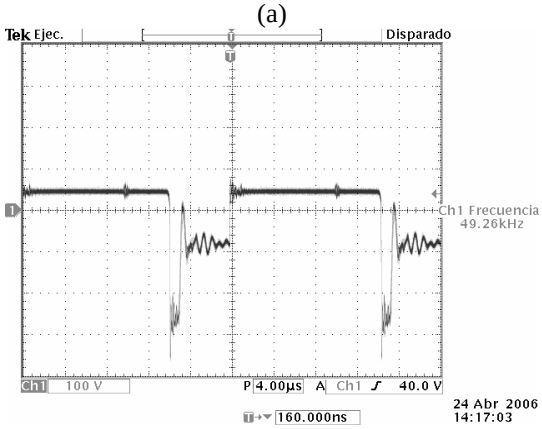

(b)

Fig. 9- (a) Voltage across the primary of the Flyback transformer – Simulation.
(b) Voltage across the primary of the Flyback transformer- Experimental. 100V/div.

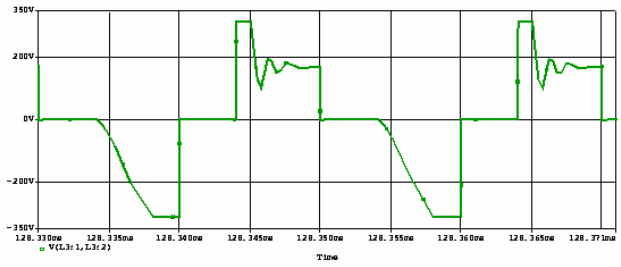

(a)

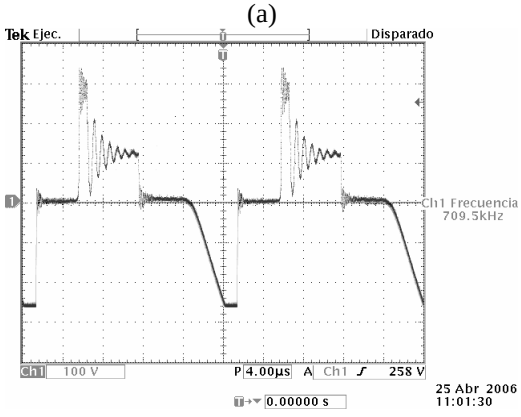

(b)

Fig. 10 - (a) Voltage across the primary of the Forward transformer – Simulation.
(b) Voltage across the primary of the Forward transformer – experimental 100V/div.

In figure 13(b) it is possible to see the efficiency of the nominal load, 86%. Being a high efficiency even when semi-dissipative voltage clamping circuits were used, this is because a part of the energy stored in the leakage and

magnetization inductance of Forward transformer is redirected towards the load through Flyback transformer.

It is evident that with the use of regenerative circuits the efficiency should be even better, since the totality of the energy of magnetization and leakage inductances of both transformers would not be lost.

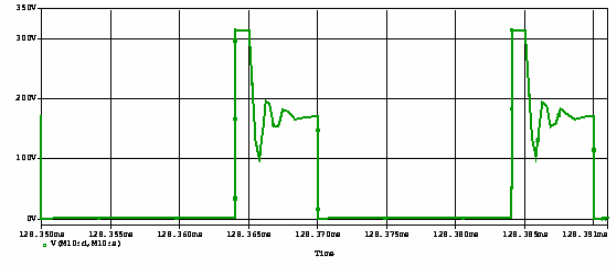

(a)

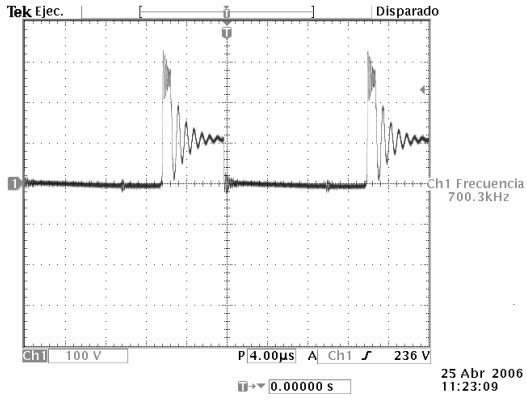

(b)

Fig. 11 - (a) Voltage across S_1 switch – simulation
(b) Voltage across S_1 switch – experimental 100V/div.

5. CONCLUSIONS

The analyzed converter in this paper is part of the family of the isolated converters with two ways of processing energy, in this case generated from Tapped-Inductor Boost Converters. The advantage of integrating two ways of processing energy is that the energy transferred to the load is divided in two magnetic cores, increasing the efficiency. These converters have the Forward and Flyback converters characteristics.

It was possible to demonstrate the good performance of the Flyback-Isolated Boost circuit, showing the main experimental waveforms and also by digital simulation (with real parameters). With this it was possible to verify that the converter was well designed.

Also were found the efficiency curves and the output characteristic of the new converter. Where is possible to see from figure 13(a) to the converter behave as a voltage source for different levels of load. From Figure13 (b) is observed that the efficiency obtained at full load was 86%, even when semi-dissipative snubbers for the switches were used. This is due to stage where the energy is directed to primary windings of the Flyback transformer and through of this to the load.

On the other hand, an important drawback of the continuous conduction mode is the presence of a zero in the right half plane (RHP) in the control-output transfer function, which is consistent with the accumulation converters. It not possible a parameter combination of the circuit in order to eliminated this zero.

Also, it was observed that this converter is too sensitive to leakage inductances of the magnetic elements (Flyback and Forward transformers), because they have a serial connection between them, adding theirs parasites inductances. Therefore, a careful analysis of the clamping circuits is necessary in order to optimize the total efficiency of the circuit. .

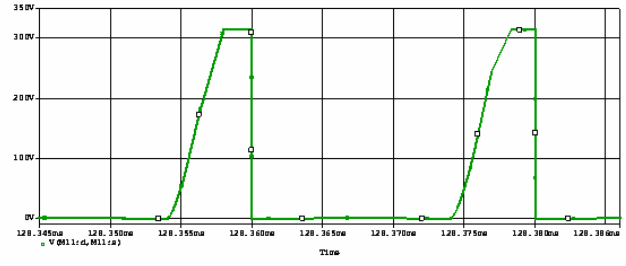

(a)

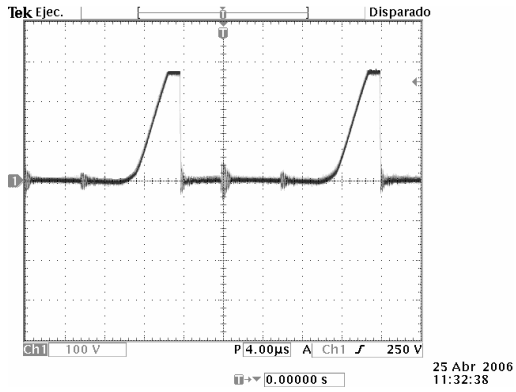

(b)

Fig. 12 - (a) Voltage across the S_2 – simulation.
(b) Voltage across the S_2 – experimental 100V/div.

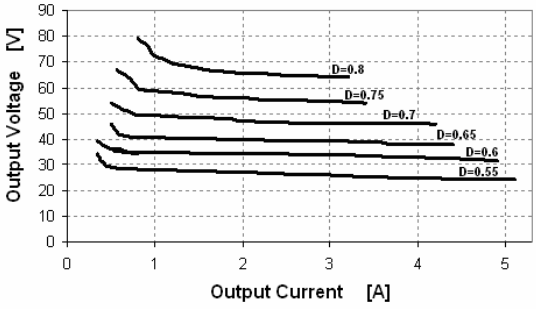

(a)

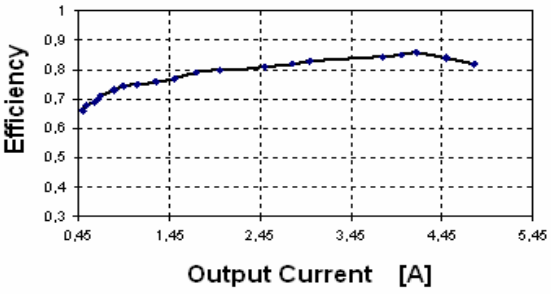

(b)

Fig.13 - (a) Output characteristic, (with N_1=N_2=6.82).
(b) Efficiency experimental

6. REFERENCES

[1] A.H. Weinberg, *"A Boost Regulator with a New Energy-Transfer Principle"*, in Proceedings os the Spacecraft Power Conditioning Electronics seminar, 1971 Record, pp.115-122.

[2] D. A. Ruiz-Caballero and I. Barbi, *"A New Flyback-Current-Fed Push-pull DC-DC Converter"*, IEEE Transaction on Power Electronics, Vol. 14 No6 November 1999, pp.1056-1064.

[3] R.D. Middlebrook, *"A Continuous Model for the Tapped-Inductor Boost Converter"*, IEEE Power Electronics Specialists Conference, 1975 Record, pp.63-79.

[4] P. Mantovanelli and I. Barbi, *"A New Current Fed, Isolated PWM DC-DC Converter"*, IEEE Transaction on Power Electronics, Vol. 11 No3 May 1996, pp.43-44.

[5] M. Rico, J. Uceda, J. Sebastian and F. Aldana, *Static and Dynamic Modeling of the Tapped-Inductors DC-to-DC Converters*, Proceeding of PESC 87, Record, pp. 281-287, 1987.

[6] G. E. Bloom and R. Severns, *Modem DC-to-DC Switch Mode Power Converters Circuits*, Van Nostrand-Reinhold, Inc, Pp 121-123, 1984.

[7] Guillermo Tapia Leiva, "Desarrollo teórico experimental de un nuevo convertidor CC-CC Boost aislado, con dos formas de procesar energía". Informe final, Pontificia Universidad Católica de Valparaíso, Chile, 2006.

[8] Julio Cesar Castro Campos, "Desarrollo teórico experimental de un nuevo convertidor aislado CC-CC, con dos formas de procesar energía". Informe final, Pontificia Universidad Católica de Valparaíso, Chile, 2004.

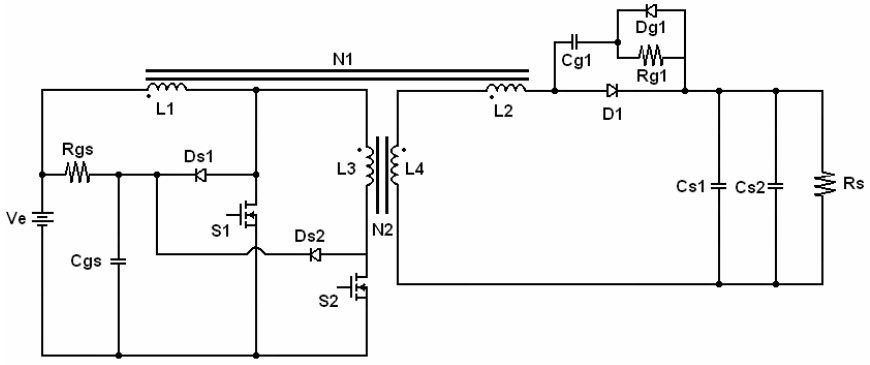

(a)

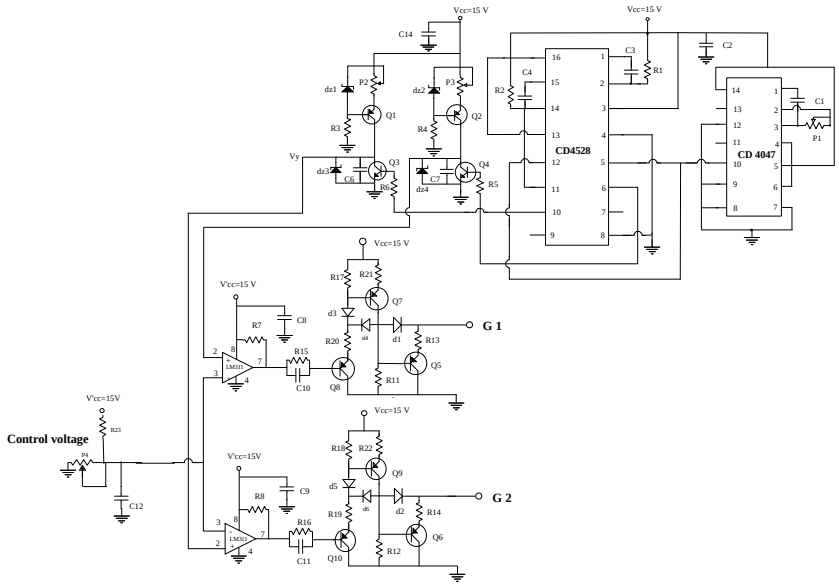

(b)

Fig. 14.- Built prototype diagram:; (a) Flyback-Isolated Boost Power circuit (b) Control Circuit